Talanta 85 (2011) 533–540

Contents lists available at ScienceDirect

Talanta

journal homepage: www.elsevier.com/locate/talanta

Selective colorimetric sensing of cysteine in aqueous solutions using silver nanoparticles in the presence of Cr^{3+}

Aswathy Ravindran, Vinayak Mani, N. Chandrasekaran, Amitava Mukherjee*

Nano-biomedicine Research Group, School of Bio Sciences & Technology, VIT University, Vellore 632014, India

ARTICLE INFO

Article history:
Received 8 March 2011
Received in revised form 8 April 2011
Accepted 11 April 2011
Available online 16 April 2011

Keywords:
Ag NPs
Colorimetric probe
Chromium ions (Cr^{3+})
Aggregation
Cysteine

ABSTRACT

We here in report an extensive study on the development of a highly facile, selective and sensitive colorimetric probe for cysteine detection using silver nanoparticles (Ag NPs). The efficacy of the process relies upon the surface plasmon resonance properties of Ag NPs and the interaction of Ag–cysteine complex with chromium ions (Cr^{3+}) in a ratio of 2:1. In the presence of Cr^{3+}, cysteine was able to induce the aggregation of Ag NPs thereby resulting in a change in yellow colour of the Ag colloid to purple. The reported probe has a limit of detection down to 1 nM which is to the best of our knowledge the lowest ever reported for the colorimetric detection of cysteine. Furthermore, a remarkable feature of this method is that it involves a simple technique exhibiting high selectivity to cysteine over other tested amino acids.

1. Introduction

Cysteine is sulfur containing non-essential amino acid and forms a dominant part of most of the peptides and proteins. High reactive nature of thiol groups makes cysteine a special amino acid as it plays an authoritative role in the most important process of protein synthesis i.e. protein folding [1]. Other important biological functions of cysteine are in detoxification and metabolic processes [2,3]. Abnormal levels of cysteine and its derivatives have been widely linked to various life threatening diseases like HIV, cancer, sepsis, ulcerative colitis and many others [4]. Hence, from the above-mentioned facts the importance of cysteine detection is well understood.

Most widely employed methods for the accurate detection of cysteine involve chromatographic techniques [5]. However various other approaches have been made for better, cheaper and less tedious detection of cysteine and its derivatives. Some of them employ the basic principles of electrochemistry, fluorescence and chemical analysis [6]. But the problem still persists regarding the sensitivity limit, cost effectiveness and tedious procedures involving significant time for analysis. With the advent of nanotechnology there has been shift of interests of the science fraternity towards developments of sensors using nanoparticles [7]. Emergence of various colorimetric biosensors has revolutionized the efforts for developing the cheapest and most sensitive and accurate sensors for biomolecule detection.

According to our thorough literature survey, most of the colorimetric detection methods have employed surface employed gold nanoparticles (Au NPs) [8–12]. Recently, Weia et al. developed a colorimetric sensor for cysteine detection using carboxymethyl cellulose-functionalized Au NPs [13]. In another approach, Chen et al. [14] used ssDNA stabilized Au NPs for colorimetric detection of cysteine. However, the main disadvantage of these approaches was their low sensitivities, in which only micro molar concentrations of cysteine was detectable; the above detection processes generally needed a rather long time and some other thiol-containing compounds could generate interference for cysteine detection.

Metal nanoparticles especially silver exhibit excellent surface plasmon resonance properties thereby providing them with extremely high extinction coefficient and strong surface plasmon resonance properties [15–18]. In this study, we report for the first time, the use of silver nanoparticles (Ag NPs) as a visual colorimetric detection probe for the highly facile, selective and sensitive detection of cysteine using chromium ions (Cr^{3+}). The addition of Cr^{3+} induces the aggregation of Ag NPs resulting in a change in the colour of the colloid from yellow to purple depending on the concentration of cysteine. The metal ions are expected to bind with the cysteine–Ag NPs through cooperative metal–ligand interactions. Cysteine of concentrations as low as 1 nM can be detected using this colorimetric format. In this context, we have shown that the interaction of the Ag NPs with cysteine in the presence of Cr^{3+} results in appreciable changes in colour and absorption properties over other amino acids tested with overall process taking less than 5 min.

---

* Corresponding author. Tel.: +91 416 2202620; fax: +91 416 2243092.
E-mail address: amit.mookerjea@gmail.com (A. Mukherjee).

0039-9140/$ – see front matter © 2011 Elsevier B.V. All rights reserved.
doi:10.1016/j.talanta.2011.04.031

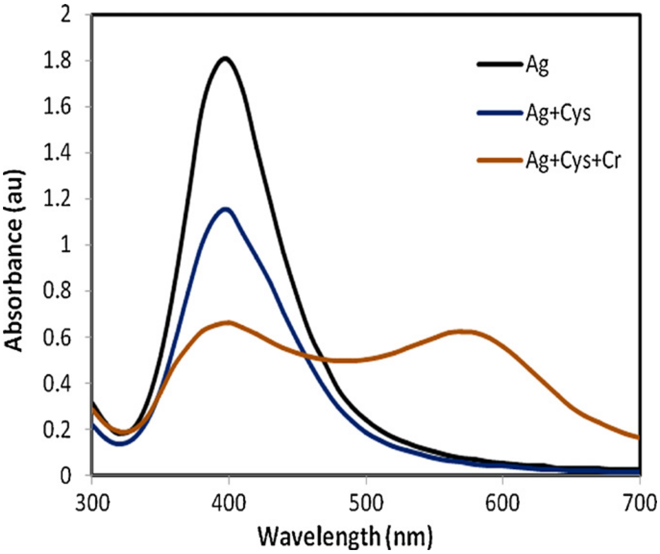

Fig. 1. UV–vis spectra of synthesized Ag NPs, before and after interaction with 10^{-3} M cysteine and 10^{-3} M Cr^{3+}.

2. Materials and methods

2.1. Chemicals

Deionized and distilled water from Mill-Q was used throughout the experiments. All the amino acids were purchased from Sigma Aldrich Co. (USA). Sodium borohydride ($NaBH_4$), sodium chloride (NaCl), tri-sodium citrate and silver nitrate ($AgNO_3$) were purchased from SD Fine Chemicals Ltd. Heavy metal salts were obtained from Himedia Laboratories Pvt. Ltd. All the heavy metal salt solutions (1 mM) used for the experiments were prepared by mixing the requisite amount of salt in Mill-Q water. Cysteine (10^{-2} M) was used as the stock solution and was serially diluted to give lower concentrations of cysteine solutions. For preparation of cysteine and other amino acid solutions distilled and deionized water was used as the solvent. Hydrochloric acid (HCl) and sodium hydroxide (NaOH) were used to adjust the pH.

2.2. Synthesis of Ag nanoparticles (Ag NPs)

All the glassware used were thoroughly washed with fresh water and then rewashed with Mill-Q water and air dried. Ag NPs were prepared according to the published Creighton's method [19] with minor modifications. Briefly, 30 ml of 2 mM sodium borohydride ice-chilled solution was mixed with 2 ml of 1% tri-sodium citrate while stirring for 5 min. 10 ml of 1 mM silver nitrate solution was added drop by drop under dark conditions without stirring. Pale yellow colour marks the end of the reaction and confirms the formation of particles.

2.3. Characterization

2.3.1. UV–vis spectroscopy

After the formation, the preliminary characterization of particles was done by UV–vis spectroscopic studies. The spectra were recorded in a UV–visible spectrophotometer (Shimadzu UV-1700, Japan) from 200 to 700 nm. Millipore water was used as blank. The spectra recorded were then replotted using Microsoft Excel.

2.3.2. Particle size analysis

The particle size range of the nanoparticles along with its polydispersity was determined using a particle size analyzer (90 Plus Particle Size Analyzer, Brookhaven Instruments Corporation). Particle size was arrived by calculating the mean hydrodynamic diameter (*z*-average mean) from the autocorrelation function of the intensity of light scattered from the particles undergoing Brownian motion. Around 3 ml of the synthesized colloid was subjected to particle size analysis to determine the hydrodynamic size of the nanoparticle.

2.3.3. Zeta potential measurements

The zeta potential of the synthesized nanoparticles was determined by means of zeta potential analyzer (90 Plus Particle Size Analyzer, Brookhaven Instruments Corporation, using Zeta Plus software). The measurement of zeta potential is based on the direction and velocity of particles under the influence of known electric field. Zeta potential values were taken to predict the nature of the electrostatic potential near the surface of the particle by mixing an aliquot of the sample with 10^{-3} M KCl solution prior to analysis.

2.3.4. Microscopy

2.3.4.1. Atomic force microscopy. The shape and structure of the Ag NPs were determined using atomic force microscopy (AFM). AFM studies were carried out by drop coating the dispersion containing the particles onto a glass slide after required reaction time and scanning at a rate of 100 mV/s in the range 50 μm × 50 μm using Nanosurf Easy Scan 2, Nanosurf Inc., USA.

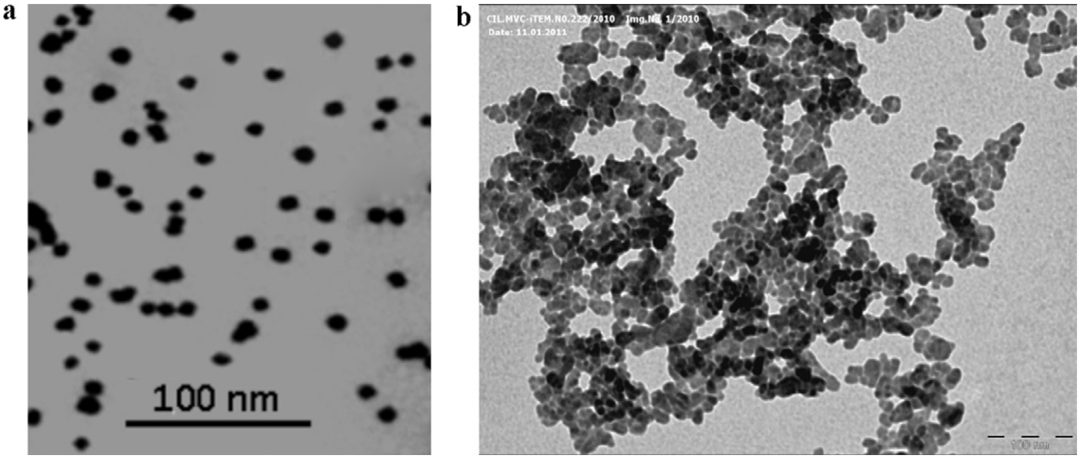

Fig. 2. TEM micrograph of (a) synthesized Ag NPs, (b) Ag NPs with 10^{-3} M cysteine in the presence of 10^{-3} M Cr^{3+}.

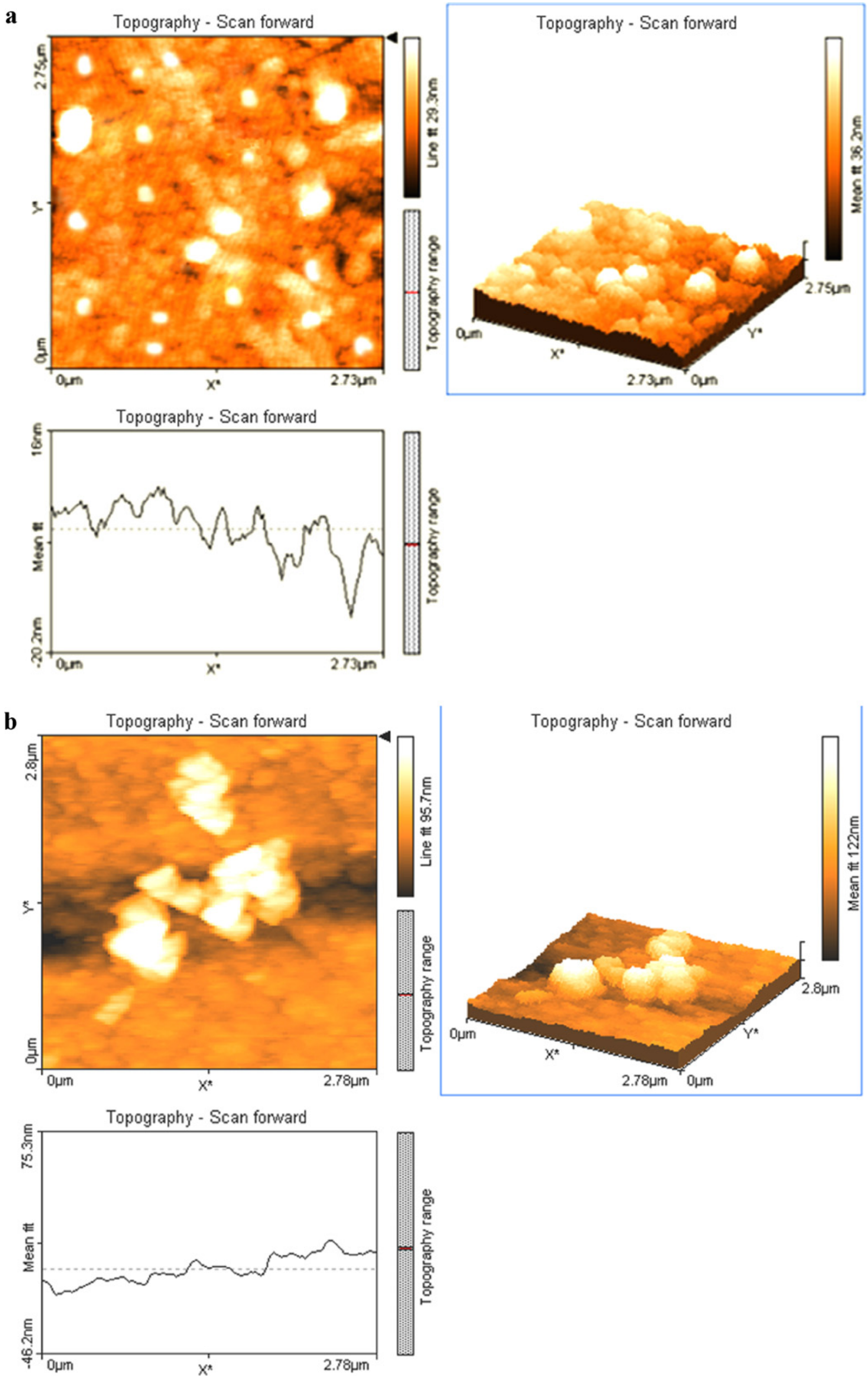

Fig. 3. Atomic force microscopic image of (a) synthesized Ag NPs, (b) Ag NPs with 10^{-3} M cysteine in the presence of 10^{-3} M Cr^{3+}.

2.3.4.2. Transmission electron microscopy. The morphology of the synthesized nanoparticles was determined by transmission electron microscopy (TEM). Samples for TEM measurements were prepared by placing a drop of test solution on the copper grid and drying it in vacuum. Transmission electron micrographs were taken using (Technai 10, Philips) operated at an accelerated voltage of 80 kV and an ultra high resolution pole piece.

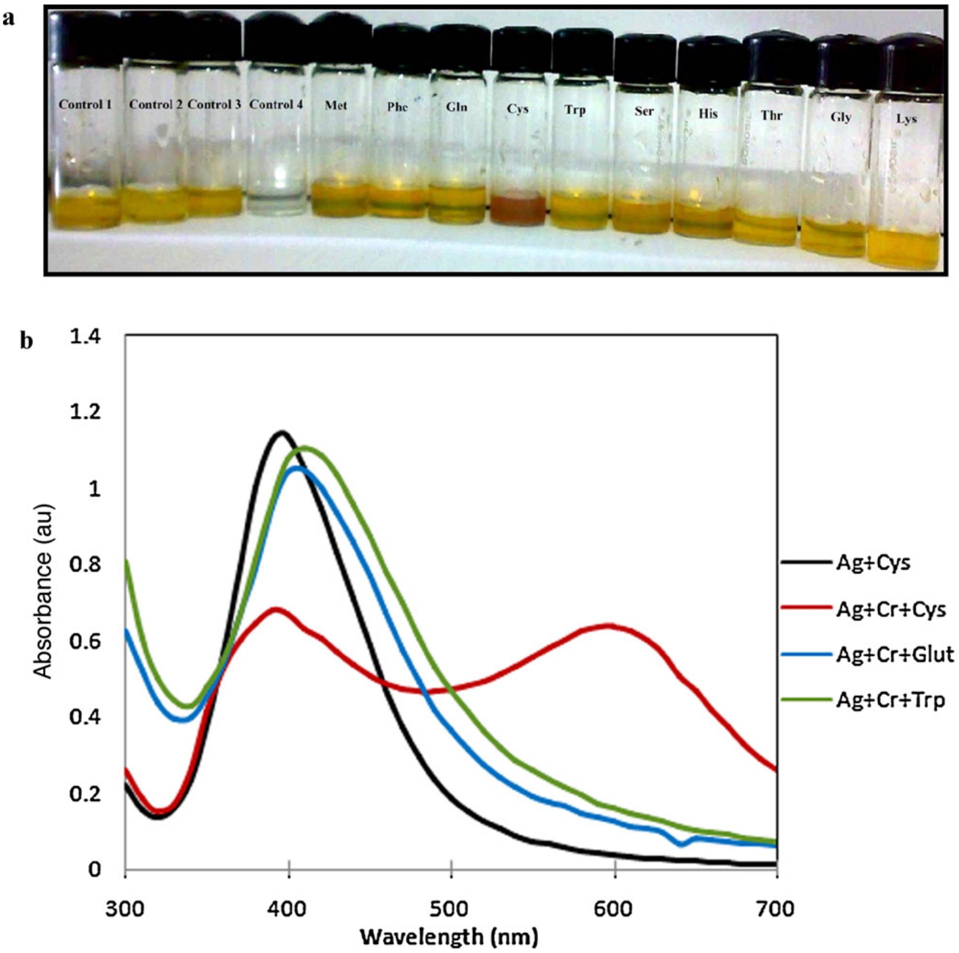

Fig. 4. (a) Photographic image of Ag NPs interacted with Cr^{3+} in the presence of different amino acids. (*Note*: Control 1 = Ag, Control 2 = Ag + cysteine, Control 3 = Ag + Cr^{3+}, Control 4 = Cr^{3+} + cysteine. Concentration of amino acids and $Cr^{3+} = 10^{-3}$ M). (b) UV–vis spectra of Ag + cysteine and Ag + amino acid + 10^{-3} M Cr^{3+} (order of amino acids (10^{-3} M): cysteine, glutathione and tryptophan respectively.)

2.4. *Colorimetric detection of cysteine*

Colorimetric detection of cysteine was carried out by first adding 250 μl of cysteine to 700 μl of freshly prepared Ag NPs and leaving it for interaction for 1 min. To the mixture 500 μl of freshly prepared Cr^{3+} (1 mM) solution was added and checked for instant colouration. Absorption spectra of the final mixture were recorded using cells with 1 cm path length. The concentration of cysteine in the solution was easily measured with the help of values of absorption ratio ($A_{590/390}$).

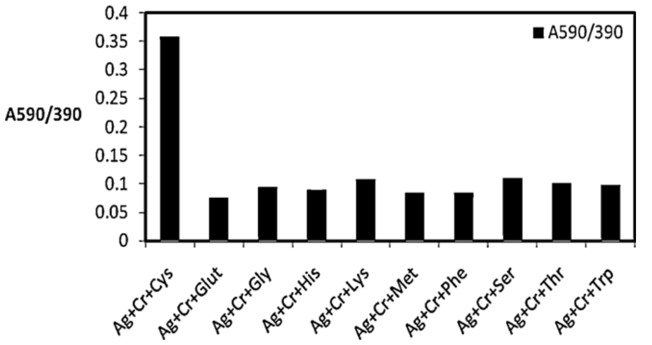

Fig. 5. Comparison of absorbance ratios (A_{590}/A_{390}) of each amino acid mixture with Ag NPs and Cr^{3+}.

All the tests were carried out in triplicate, and mean values of the results were reported. The experimental error limit was strictly kept within ±5%.

3. Results and discussion

3.1. *Characterization of the particles before and after interaction*

The as-synthesized colloidal Ag NPs were subjected to UV–vis spectroscopy. The particles gave a strong plasmon resonance band at 390 nm. On interacting with cysteine in the presence of Cr^{3+} the particles immediately aggregated with an intense colour change from yellow to purple. The result was consistent with the red shift of UV–vis spectra. The plasmon band centered on 390 nm shifted to the right forming a second peak at 590 nm (Fig. 1). This second peak could be ascribed to the complex formed due to the aggregation of the particles. In order to know the microstructure of the Ag NPs before and after interacting with cysteine, TEM and AFM were performed. It is to be noted from the transmission microscopic images that in the absence of cysteine and Cr^{3+}, the Ag NPs formed were spherical and monodispersed in nature with an average particle size of 10–15 nm while in its presence Ag NPs formed large aggregates of 50–60 nm (Fig. 2a and b). The atomic force microscopic images of Ag NPs revealed that the particles were spherical in nature and well dispersed with an average particle size between 10 and 20 nm (Fig. 3a). The Ag/cysteine–Cr^{3+} interacted samples were also subjected to atomic force microscopy to reveal the three

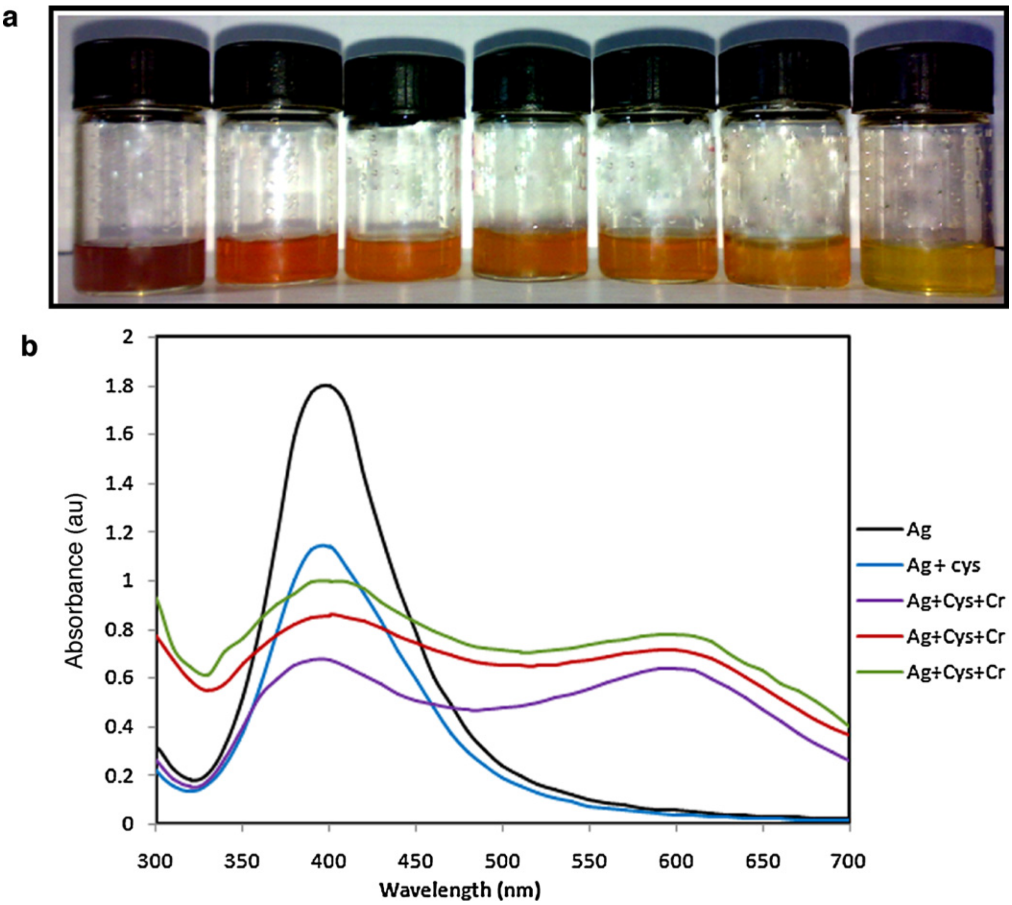

Fig. 6. (a) Photographic images of Ag NPs under different concentrations of cysteine (1×10^{-3}–1×10^{-9} M) respectively after the addition of 10^{-3} M Cr^{3+} solution. (b) UV–vis spectra of synthesized Ag NPs containing different concentrations of cysteine (1×10^{-3} M, 1×10^{-6} M, 1×10^{-9} M) after the addition of 10^{-3} M Cr^{3+}.

dimensional structure and the morphological changes following the interaction of the particles with Cr^{3+}. The microscopic studies revealed the formation of large flocs (size 55–60 nm) due to the aggregation of the particles as seen in Fig. 3b. DLS and zeta potential readings were also taken to corroborate with the spectroscopic and microscopic findings. The average hydrodynamic diameter of the particle was 55.2 nm while the mixtures of colloidal silver solution in the presence of cysteine and Cr^{3+} evidenced a relatively high degree of poly dispersion with an increase in size of particles to 152 nm after 10 min of interaction. The colloidal silver solution gave a mean zeta potential value of −30.71 mV, which is usually considered as the limit for colloidal systems [20] while in the mixture obtained after interaction with cysteine and Cr^{3+}, the zeta potential values were less negative (−19.63 mV), indicating a concomitant decrease in colloidal stability upon aggregation.

3.2. *Sensitivity and selectivity of the analytical process*

In order to check the selectivity of cysteine over other amino acids the experiment was performed as described in Section 2.3, but instead of cysteine, 10^{-3} M of other amino acid solutions (phenylalanine, glutamine, tryptophan, serine, histidine, threonine, lysine, glycine and methionine) were individually added in the same ratio as of cysteine. The results obtained clearly indicate that except cysteine no other amino acids exhibited a colour change (Fig. 4a). In addition, UV–vis data did not reveal the presence of a peak at around 590 nm in the other amino acids except cysteine. The spectral changes exhibited by some selected amino acids (cysteine, glutathione and tryptophan) are given in Fig. 4b (a detailed UV–vis spectrum of 10 interacted amino acids including cysteine is given in Fig. S1 (supplementary information)). The absorption ratio (A_{590}/A_{390}) of Ag NPs in the presence of 10^{-3} M cysteine and 10^{-3} M of other amino acids is shown in Fig. 5.

Further, to check the sensitivity level of this method, different concentrations of cysteine solutions ranging from 10^{-3} M to 10^{-9} M were interacted with Ag NPs in the presence of cysteine. A fine gradation in the colour development was recorded from intense purple to feeble pink as the concentration of cysteine in the solution decreased to nanomolar level (Fig. 6a). Some significant spectral changes for cysteine concentrations (10^{-3} M, 10^{-6} M, 10^{-9} M) recorded before and after interaction are shown in Fig. 6b (detailed UV–vis spectra of different concentrations of cysteine interacted with Ag NPs and Cr^{3+} are given in Fig. S2 (supplementary information)). A linear correlation was recorded up to 10^{-9} M as it can be seen from the graph showing the ratio of absorbance ($A_{590/390}$) versus logarithm of cysteine concentration as shown in Fig. 7. Hence, the present limit of detection of this sensor is 1 nM. To the best of our knowledge as of now this is the lowest sensing limit recorded for the visual colorimetric detection of cysteine using Ag NPs.

3.3. *Possible mechanism for the detection of cysteine using Ag NPs as a colorimetric probe*

The synthesis of Ag NPs was achieved by citrate reduction method to yield monodispersed particles. Ag NPs (10 nm) in aqueous solution are stabilized against aggregation due to the negatively charged citrate ions electrostatically repelling against Van der

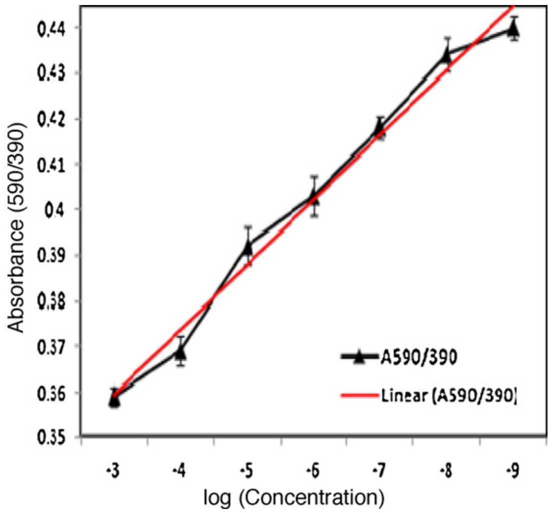

Fig. 7. Calibration curve of $A_{590/390}$ against $\log_{10}$ of cysteine concentration in Ag NPs containing 10^{-3} M Cr^{3+} (graph shows linear relationship between $A_{590/390}$ against $\log_{10}$ of cysteine).

Waals attraction between Ag NPs [21]. The thiol group of cysteine exhibits intriguing reactivity with Ag NPs by binding onto the surface of the silver particles through the sulfur atom [22] and the Ag NPs are thus functionalized with cysteine. On the other hand, cysteine can bind to Cr^{3+} by coordinating with its acidic (COOH) and basic (NH_2) functional groups [23]. Thus each Cr^{3+} forms complexes with two cysteine molecules as shown schematically in Fig. 8. Thus, Cr^{3+} can act as cross-linking agent for pairs of cysteine-coated Ag NPs, thereby inducing the aggregation of Ag NPs. This causes a rapid, yellow-to-purple colour change. We just make use of this property to design our sensor for cysteine. The Ag NPs colloidal solution with Cr^{3+} in the absence of cysteine is yellow, while the Ag NPs colloidal solution with Cr^{3+} in the presence of cysteine is purple. We also found that the control experiments with other amino acids did not show colour change.

3.4. Optimization of the assay conditions

To investigate the effect of various heavy metals on the Ag–cysteine complex during the development of the experiment various heavy metal salt solutions were added to the Ag–cysteine complex. Upon interaction with the complex it was observed that Cr^{3+} gave deep violet colour instantly with a prominent second UV peak at nearly 590 nm while other salt solutions like Fe^{2+}, Cu^{2+},

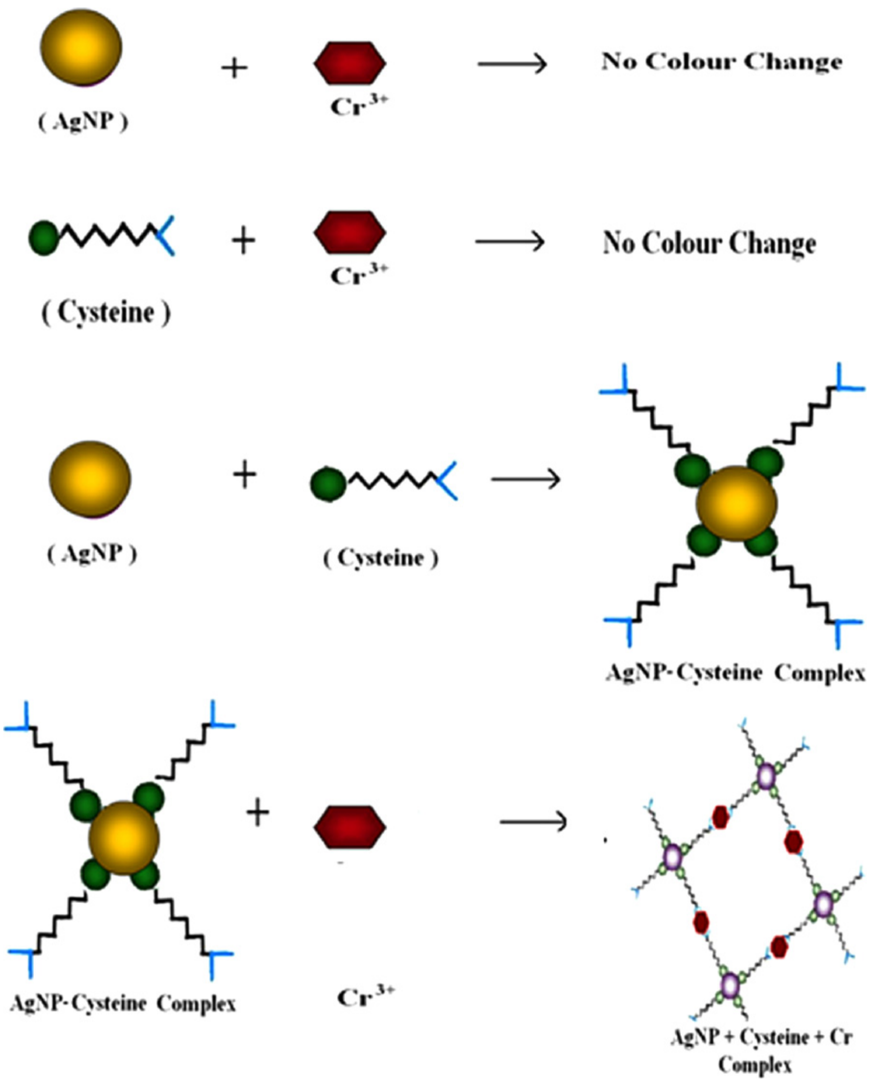

Fig. 8. Schematic representation of the mechanism of cysteine detection.

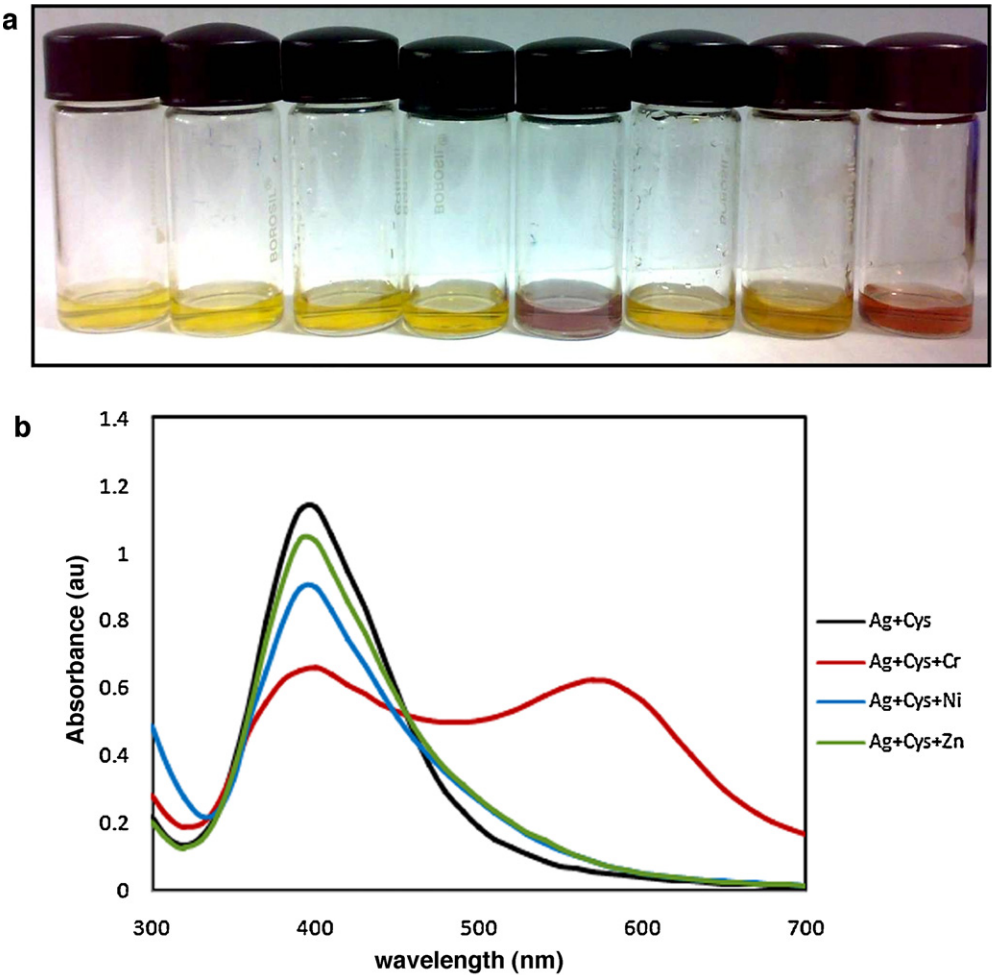

Fig. 9. (a) Photographic image of Ag/cysteine mixture interacted in the presence of different heavy metals (various heavy metals (from left to right in order): Control (Ag NPs), Ag + cysteine, Ag + cysteine + heavy metal (Fe^{2+}, Cu^{2+}, Cr^{3+}, Ni^{2+}, Pb^{2+} and Zn^{2+} respectively). *Note*: Concentration of cysteine = heavy metals = 10^{-3} M). (b) UV–vis spectra of synthesized Ag NPs colloidal solution, before and after interaction with 10^{-3} M cysteine and 10^{-3} M heavy metal ions (Cr^{3+}, Ni^{2+} and Zn^{2+}).

Ni^{2+} and Pb^{2+} did not show any colour change (Fig. 9a). The UV–vis spectra of some of the heavy metals (Cr^{3+}, Ni^{2+} and Zn^{2+}) interacted with Ag–cysteine mixtures are given in Fig. 9b (a detailed spectrum for various heavy metals with Ag–cysteine is given in Fig. S3, supplementary information). Zn^{2+} gave a light pink colour (Fig. 9a) but unlike Cr^{3+} there was no second prominent UV peak caused due to the complex formed by Ag–cysteine and Cr^{3+} (Fig. 9b). Moreover, when interacted with lower concentrations of cysteine there was no sign of colour change. Hence, Cr^{3+} was selected for further experiments.

3.5. *Detection of cysteine in artificial samples*

In order to verify the performance of the probe for detection of cysteine in practical applications, the possible interferences of other amino acids as stated above were mixed together with cysteine in the tested samples. The results indicated that the interference ions did not affect the determination of cysteine. Therefore, these excellent properties substantially enable the present probe work in the practical application for on-site, real-time detection of cysteine.

4. Conclusion

In summary we have developed a facile, sensitive and selective colorimetric probe for the on-site and real-time detection of cysteine using Ag NPs as a colorimetric probe. This assay is based on the distance dependent optical properties of Ag NPs and the interaction of cysteine:Cr^{3+} in a ratio of 2:1. In the presence of Cr^{3+}, cysteine was able to induce the aggregation of Ag NPs thereby resulting in a change in yellow colour of the Ag colloid to purple. The assay described in this work is easily detectable with the naked eye or by using a UV–vis spectrophotometer. The reported probe has a limit of detection of 1 nM which is to the best of our knowledge the lowest ever reported for the colorimetric detection of cysteine using non-functionalized Ag NPs. Furthermore, one of the remarkable features of this method is that it exhibits high selectivity to cysteine over other tested amino acids and other thiol compounds (such as glutathione).

Acknowledgement

We are extremely thankful to Dr. Sukumar of Madras Veterinary College, Chennai, for providing instrumental support for microscopic studies.

Appendix A. Supplementary data

Supplementary data associated with this article can be found, in the online version, at doi:10.1016/j.talanta.2011.04.031.

References

[1] W.H. Wang, O. Rusin, X.Y. Xu, K.K. Kim, J.O. Escobedo, S.O. Fakayode, K.A. Fletcher, M. Lowry, C.M. Schowalter, C.M. Lawrence, F.R. Fronczek, I.M. Warner, R.M. Strongin, J. Am. Chem. Soc. 127 (2005) 1594–15958.
[2] W. Droge, V. Hack, R. Breitkreutz, E. Holm, G. Shubinski, E. Schmid, D. Galter, BioFactors 8 (1998) 97–102.
[3] L.P. Osman, S.C. Mitchell, R.H. Waring, Sulfur Rep. 20 (1997) 155–172.
[4] W. Droge, E. Holm, FASEB J. 11 (1997) 1077–1089.
[5] M.L. Lunar, S. Rubio, D. Bendito, M.L. Carreto, C.W. McLeod, Anal. Chim. Acta 337 (1997) 341–349.
[6] J. Wanga, Y.F. Li, C.Z. Huanga, T. Wua, Anal. Chim. Acta 626 (2008) 37–43.
[7] W. Yang, J.J. Gooding, Z. He, Q. Li, G. Chen, J. Nanosci. Nanotechnol. 7 (2007) 712–716.
[8] F.X. Zhang, L. Han, L.B. Israel, J.G. Daras, M.M. Maye, N.K. Ly, C.J. Zhong, Analyst 127 (2002) 462–465.
[9] H. Guan, P. Zhou, X. Zhou, Z. He, Talanta 77 (2008) 319–324.
[10] Z.S. Wu, S.B. Zhang, M.M. Guo, C.R. Chen, G.L. Shen, R.Q. Yu, Anal. Chim. Acta 584 (2007) 122–128.
[11] A. Sugunan, C. Thanachayanont, J. Dutta, J.G. Hilborn, Sci. Technol. Adv. Mater. 6 (2005) 335–340.
[12] Y.P. Zhanga, J. Chena, L.Y. Baib, X.M. Zhoub, L.M. Wanga, J. Chin. Chem. Soc. 57 (2010) 972–975.
[13] X. Weia, L. Qia, J. Tan, R. Liu, F. Wanga, Anal. Chim. Acta 671 (2010) 80–84.
[14] Z. Chen, S. Luo, C. Liu, Q. Cai, Anal. Bioanal. Chem. 395 (2009) 489–494.
[15] T.C. Prathna, N. Chandrasekaran, A.M. Raichur, A. Mukherjee, Colloids Surf. B 82 (2011) 152–159.
[16] A. Ravindran, A. Singh, A.M. Raichur, N. Chandrasekaran, A. Mukherjee, Colloids Surf. B 76 (2010) 32.
[17] H. Li, Y. Bian, Nanotechnology 20 (2009) 145502 (6 pp.).
[18] H. Li, Z. Cui, C. Han, Sens. Actuators B 143 (2009) 87–92.
[19] N.R. Jana, L. Gearheart, C.J. Murphy, Chem. Commun. 7 (2001) 617.
[20] R.J. Hunter, Zeta Potential in Colloid Science – Principles and Applications, Academic Press, UK, 1988.
[21] A. Ono, H. Togashi, Angew. Chem. Int. Ed. 43 (2004) 4300–4302.
[22] K. Uvdal, P. Bodo, B.J. Liedberg, Colloid Interface Sci. 149 (1999) 162–173.
[23] A.C. Liu, D.C. Chen, C.C. Lin, H.H. Chou, C.H. Chen, Anal. Chem. 71 (1999) 1549–1552.